Quench Propagation and Protection Analysis of the ATLAS Toroids

A.V. Dudarev[1], A.V. Gavrilin[1], H.H.J. ten Kate[1], D. E. Baynham[2], M. J. D. Courthold[2] and C. Lesmond[3]

[1] CERN, ATLAS Magnet Project, EP Division, Geneva 23, CH-1211, Switzerland
[2] Rutherford Appleton Laboratory, UK, [3] CEA/Saclay, France

***Abstract* – The ATLAS superconducting magnet system consists of the Barrel Toroid, two End-Cap Toroids and the Central Solenoid. However, the Toroids of eight coils each are magnetically separate systems to the Central Solenoid. The Toroids are electrically connected in series and energized by a single power supply. The quench protection system is based on the use of relatively small external dump resistances in combination with quench-heaters activated after a quench event detection to initiate the internal dump of stored energy in all the coils. A rather strong quench-back effect due to eddy-currents in the coil casings at the transport current decay is beneficial for the quench protection efficiency in the event of heater failures. The quench behaviour of the ATLAS Toroids was computer simulated for normal operation of the quench protection system and its complete non-operation (failure) mode.**

I. INTRODUCTION

The magnet system of the ATLAS Toroids consists of the Barrel Toroid (BT) and two End-Cap Toroids (ECTs) with overall dimensions of 20 m diameter and 25 m length. The stored energy of the system is about 1.4 GJ at the rated current of 20 kA, see Table I, [1]. Each Toroid consists of 8 coils, and each coil of rectangular shape includes two double pancakes embedded in a massive aluminium-alloy casing (RRR≅2), see Fig. 1. The pancake windings are wound with a Rutherford type *Cu/NbTi* composite superconductor strongly stabilized with pure aluminium in a rectangular shape. The conductors for the BT and ECT are slightly different in size and current carrying capacity [1], see Table I. In spite of the fact that each Toroid has 8 coils, it will not be sectioned electrically, but all coils are connected in series. This avoids an uneven redistribution of the current between coils under quench and in doing so it excludes any mechanical overloads due to a disbalance of forces.

TABLE I
MAIN CHARACTERISTICS OF THE ATLAS TOROIDS

Characteristic	BT	ECT
Number of coils	8	2 x 8
Self-inductance	5.14 H	2.06 H
Operating current	20 kA	20 kA
Stored energy	1030 MJ	410 MJ
Run-up voltage	16 V	16 V
Busbar + current leads resistance	210 μΩ	240 μΩ
Operating peak field	3.9 T	4.0 T
Critical current @ 4.5K & peak field	> 55 kA	> 64 kA
Conductor size	57x12 mm²	41x12 mm²
Conductor length	54 km	26 km

Manuscript received September 26, 1999
A.V. Dudarev e-mail: Alexey.Dudarev@cern.ch

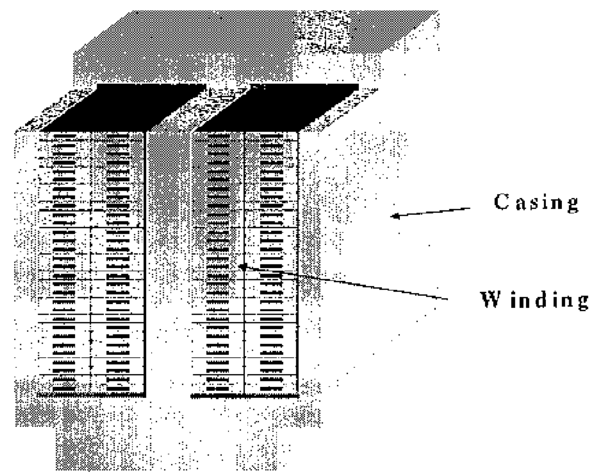

Fig. 1 Segment of the BT coil. Full cross-section of the winding (both the double pancakes) in the casing. View on the turns.

It is common knowledge that for such a large magnet system, the best way to diminish the maximum temperature and internal voltage is to distribute the stored energy uniformly, because without that a fast discharge would require a high dump resistance and hence high voltage in the circuit. The quench protection system of the ATLAS Toroids will use relatively small dump resistances and special quench-heaters embedded in each double pancake of each coil [1]. The heaters will also guarantee the magnet system discharging at low transport current during ramping.

Here, the most simple electrical scheme is considered by which the Toroids and in fact all their coils are connected in series and energized by a single power supply. The magnet system quench behaviour is computer simulated in the cases of complete non-operation of the quench protection system and when this system is triggered under normal operation.

II. NORMAL ZONE PROPAGATION

Special for a normal zone travelling in a composite superconductor having a thick aluminium stabilizer is the rather slow electromagnetic diffusion process into the stabilizer [2,3]. The transport current ejected from the superconducting filaments into the copper matrix of strands can not penetrate at once into the full section of stabilizer. For example, the characteristic time scale of the current diffusion into the

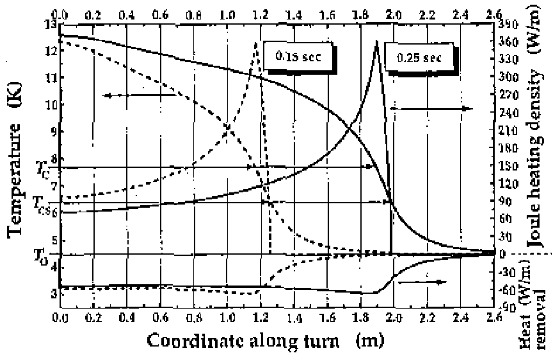

Fig. 2 Instant distributions of the temperature, Joule heating density and heat removal efficiency along a turn of the BT coil winding. Fixed current 20.5 kA, magnetic field 3.85 T.

aluminium stabilizer of the BT conductor is about 1 s, for the ECT conductor – somewhat less. The difference in specific stored energy in the cases where the transport current flows within the strands only and where it is uniformly distributed over full cross-section of the conductor comes to a few tens of Joules per meter of conductor. This relatively high initial energy density is sufficient to transfer the conductor into the normal state and then to increase its temperature by several degrees. This energy transferred into Joule heating is non-uniformly distributed over the cross-section of the conductor and this distribution varies with time. Consequently, the diffusion process has to be taken into account through a proper model. In our recent computations, a rather simple, but effective model as explained in work [3] was used. The computation results show that the lion's share of the "extra energy" is released just in the vicinity of the *ns*-boundary, where the diffusion process is in the opening stage, as may be inferred from Fig. 2. This inevitably leads to a considerable increase of the normal zone velocity as opposed to the case where the characteristic time scale of the diffusion is assumed to come close to zero.

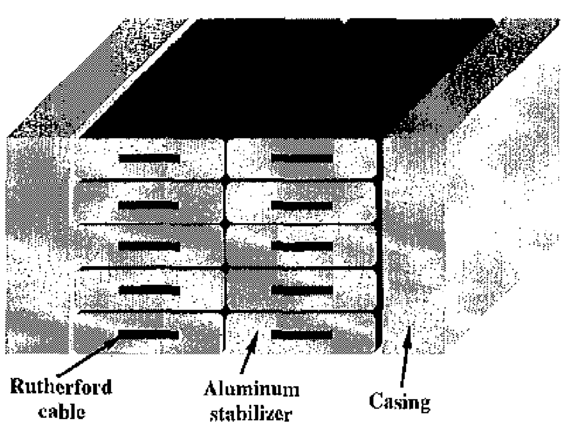

Fig. 3 Small section of the Toroid coil, the double pancake in the casing. Sketch.

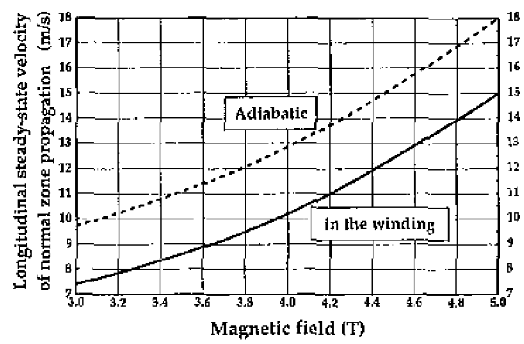

Fig. 4 Dependence of the propagation velocity along the ECT conductor on magnetic field at the rated current of 20 kA.

To determine the normal zone propagation velocity along the turns of the windings of the BT and ECT coils, a 3D model for the double pancake section was used (Fig. 3). The transient transverse heat conduction through the insulation between the turns as well as between the turns and the casing, and also the electromagnetic diffusion process are correctly included. The 3D non-linear transient heat problem is numerically solved using the finite difference method. This approach enabled the curves given in Fig. 2 to be obtained as well as the results shown in Fig. 4. Referring to Fig. 4, the longitudinal propagation velocity in the ECT coil winding is roughly 30% lower than the adiabatic velocity due to the transient transverse heat transfer (practically the same for the BT). Nevertheless, for the ECT, the steady-state velocity still is about 10 m/s at the peak field of 4 T at 20 kA. This implies that the coil winding normalization time in the longitudinal direction is about 2-3 s, only slightly influenced by the magnetic field distribution. In the BT coil winding, the longitudinal velocity approximates 7 m/s at the peak field of 3.85 T, and the longitudinal normalization time is close to 6-7 s.

To determine the transverse propagation characteristics, a 2D model is used instead. The longitudinal heat conduction is neglected, because its influence on the transverse propagation velocity is assumed to be rather weak. This minor simplification enables with the same computation capacity to consider the full cross-section of the coil winding (Fig. 1), and even cross-sections of several coils at once.

The normalization time of the BT or ECT coil winding cross-sections depends on details of the normal zone initiation. According to the results obtained, in the worst case of a normal zone origination at one of the lowermost turns of one double pancake, the transverse normalization time for the BT coil winding approximates 8 s at 3.85 T and 20 kA. However, when, as is planned, a 1mm thick pure aluminium sheet on each of the four outside faces of the double pancake between the casing and winding is used, this time could be decreased down to 6-6.5 s. The transverse normalization of the ECT coil winding takes about 5 s at 4 T @ 20 kA. When the real field distribution is taken into account instead of a certain average field, the computed normalization times increase by

~ 30%. In the case of a simultaneous normal zone initiation by the heaters in both the double pancakes, the transverse normalization time is almost halved.

Thus, it is concluded that the BT and ECT coil winding normalization is within the 10 s time frame which is an order of magnitude shorter than the easily estimated characteristic time of the current decay in the whole magnet system under quench. It means that in the computer simulation of a quench event in this magnet system, it is possible to consider each coil in the 2D approximation correctly and to make rather solid estimates of the maximum temperature and internal voltage. In such a simulation, as performed, the heat equations are solved together with the circuit equations and include eddy current generation effect in the coil casings due to the transport current decay.

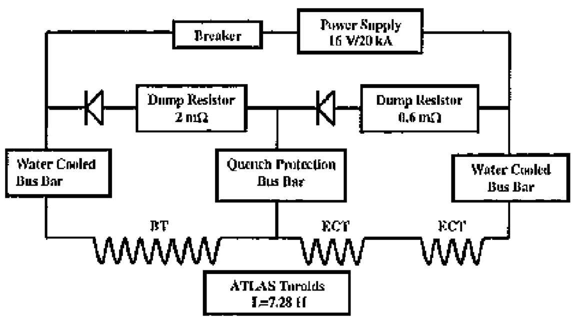

Fig. 5 The principle power circuit of the ATLAS Toroids magnet system under normal operation.

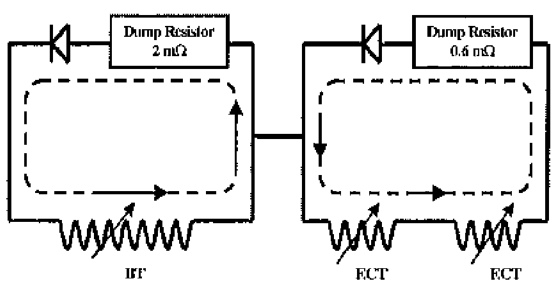

Fig. 6 Electrical scheme of the ATLAS Toroids in the fast discharge mode.

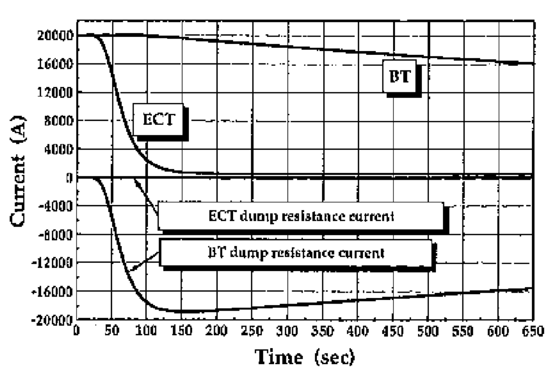

Fig. 7 Current decay in the ECTs and BT in the case of complete non-operation of the quench protection system; the ECTs under quench.

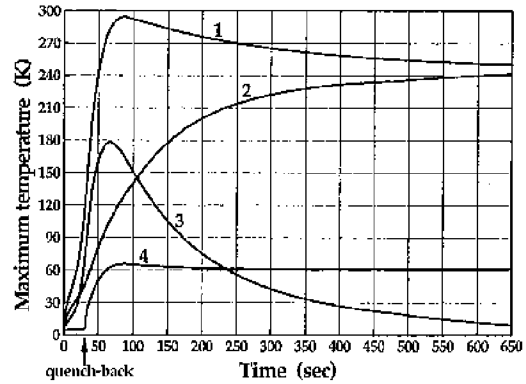

Fig. 8 Maximum temperature in the ECT coils under quench in the case of complete non-operation of the quench protection system.
1 – quenched coil winding,
2 - quenched coil casing,
3 – temperature gradient between the winding and casing of quenched coil,
4 – other 15 coil windings .

III. Quench Simulation Results

The principle electrical circuit under study and corresponding to normal operation of the ATLAS Toroids is shown in Fig. 5. Quench event detection has to cause the heaters activation and a change-over from the normal operation mode to the fast discharge mode (Fig. 6) as a result of a change of state of the breaker. In the fast discharge mode, there practically exist two circuits, the first one – for the BT, the second – for the ECTs. These circuits are inductively coupled, but this coupling is very weak, as the mutual inductance between ECTs and BT is only 0.07 H, whereas the self-inductances of the BT and ECTs are 5.14 H and 2.06 H, respectively.

In the event of a quench, the two limiting cases are considered and simulated. The first case is the worst one where the quench detection and switch system unpredictably and completely fails and the magnet system remains in the normal operation mode with the power supply in service (the maxi-

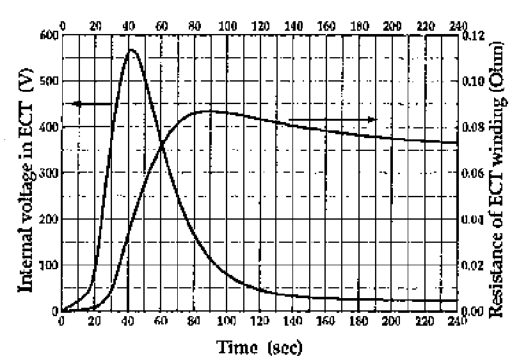

Fig. 9 Internal voltage in the ECT and resistance of the ECT winding in the case of complete non-operation of the quench protection system.

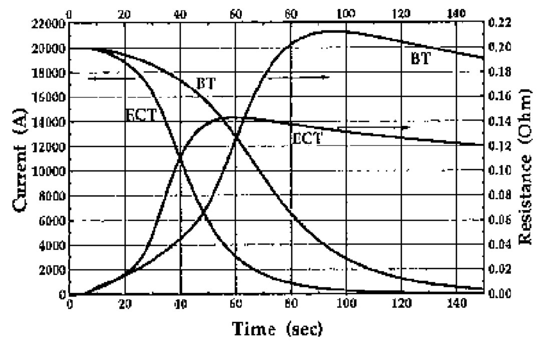

Fig. 10 Current decay and resistance of the windings of the BT and ECTs under normal operation of the quench protection system.

mum voltage 16 V), see Fig. 5. In the second case, the magnet system successfully goes on to the fast discharging (Fig. 6) with 5 s delay. In both the cases a normal zone is initiated at one of the lowermost turns of one pancake in *one* coil of the ECT that is the most severe initial condition.

The computation results corresponding to the first case are given in Figs. 7-9. As illustrated, the current in the ECTs decays mainly because of a rather fast rise of the quenched coil resistance, while no current flows through the external dump resistance of the ECTs due to the diode (Fig. 5). The current decay leads to a quench initiation in the other 15 coils of the ECTs due to eddy current generation in the casings (the quench-back) a half minute after the quench has started in the first coil (Fig. 8). As a result, the ECTs discharge accelerates.

At the same time, the BT coil windings remain superconducting, because the rising negative current through the BT dump resistance almost balances out the transport current decay in the whole circuit, see Fig. 7. A very slow discharge of the BT takes place with a rate being insufficient to have the quench-back effect as in the ECTs.

Despite the fact that the BT coil windings are kept superconducting, the opposite could vastly accelerate the whole

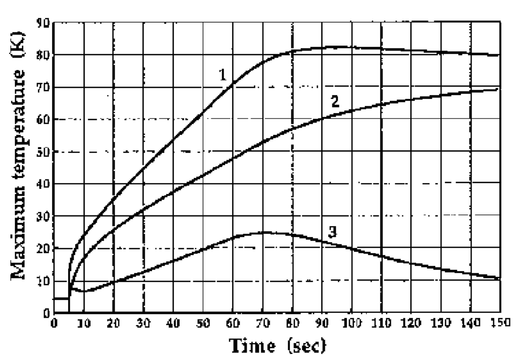

Fig. 11 Maximum temperatures in the BT under normal operation of the quench protection system.
1 – BT coil windings, 2 – BT coil casings,
3 – temperature gradient between the winding and casing.

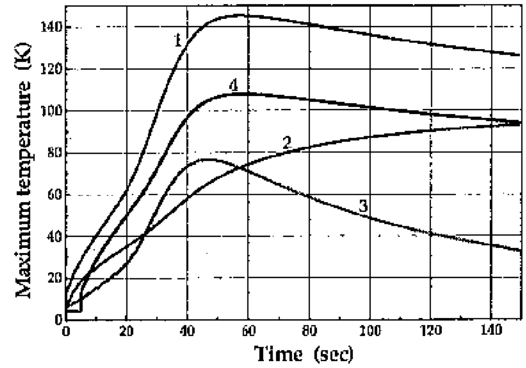

Fig. 12 Maximum temperatures in the ECT coils under normal operation of the quench protection system.
1 – quenched coil winding, 2 – quenched coil casing, 3 – temperature gradient between the winding and casing, 4 – other 15 coil windings.

magnet system discharging and does nothing but improve the situation, the maximum temperature of the quenched coil of the ECT turns out to be about only 300 K, see Fig. 8. The maximum internal voltage does not exceed 600 V, see Fig. 9.

The results corresponding to the case of normal operation of the quench protection system are shown in Figs. 10-12. In this case, the maximum temperatures of the BT and ECT windings are moderate, ~85 K and ~145 K, respectively. The maximum internal voltages in the BT and ECT are negligible.

IV. Conclusions

The quench behaviour of the ATLAS Toroids magnet system energized by a single power supply was numerically analyzed in the case of complete non-operation of the quench protection system and in normal operation of this system. In the first case, the magnet system proved itself as a self-protected one, no over-heating nor over-voltage. Further, it is shown that normal operation of the quench protection system reduces the maximum temperature of the Toroids coils at least by half and minimizes the internal voltages.

References

[1] Ten Kate H "The Superconducting Magnet System for the ATLAS Detector" *This Conference* 1999
[2] Huang X Eyssa Y Hilal M *Adv. Cryog. Eng.* 1993 **53** 155-163
[3] Gavrilin A Yanagi N Satoh S Motojima O *Adv. In Superconductivity XI (Proc. of ISS'98, November, 1998, Fukuoka)* 1999 **2** 1447-1450